Heliyon 9 (2023) e21461

Contents lists available at ScienceDirect

Heliyon

journal homepage: www.cell.com/heliyon

# *In-vitro* investigation on the biological activities of squalene derived from the soil fungus *Talaromyces pinophilus*

Meghashyama Prabhakara Bhat [a], Muthuraj Rudrappa [a], Anil Hugar [a], Pooja Vidyasagar Gunagambhire [a], Raju Suresh Kumar [b,*], Sreenivasa Nayaka [a,**], Abdulrahman I. Almansour [b], Karthikeyan Perumal [c]

[a] *P.G. Department of Studies in Botany, Karnatak University, Dharwad, 580001, Karnataka, India*
[b] *Department of Chemistry, College of Science, King Saud University, P.O. Box. 2455, Riyadh, 11451, Saudi Arabia*
[c] *Department of Chemistry and Biochemistry, The Ohio State University, 151 W. Woodruff Ave, Columbus, OH, 43210, USA*

ARTICLE INFO

*Keywords:*
*Talaromyces pinophilus*
Antibacterial activity
Squalene
Candidicidal activity
Anticancer activity
Human blood cancer

ABSTRACT

The consistent increase in multidrug resistance among pathogens and increased cancer incidence are serious public health concerns and threaten humans by killing countless lives. In the present study, *Talaromyces pinophilus* CJ15 was characterized and evaluated for its antibacterial, candidicidal and cytotoxic activities. The selected isolate *Talaromyces pinophilus* CJ15 with 18S rRNA gene sequence of 1021 base pairs exhibited antifungal activity on plant pathogens via dual culture. The GC-MS profiling of crude extract illustrated the existence of many bioactive macromolecules which include squalene belonging to the terpenoids family. The biological macromolecules in the bioactive fraction of CJ15 exhibited increasing antibacterial activity with an increase in concentration such that the highest activity was recorded against *Shigella flexneri* with 15, 18, 20, and 24 mm inhibition zones at 25, 50, 75 and 100 μl concentrations, respectively. The squalene, having a molecular weight of 410.718 g/mol, displayed candidicidal activity with a right-side shifted log phase in the growth curve of all the treated *Candida* species, indicating delayed exponential growth. In cytotoxic activity, the extracted squalene exhibited an $IC_{50}$ concentration of 26.22 μg/ml against JURKAT cells and induced apoptosis-induced cell death. This study's outcomes encourage the researchers to explore further the development of new and improved bioactive macromolecules that could help to prevent infections and human blood cancer.

## 1. Introduction

The abrupt industrialization and environmental decline accelerate the utilization of viable land for rearing, most of which is irreparable to be used for farming, horticultural production and terrestrial ecosystems [1–3]. Soil is a tremendous source of microorganisms, and microorganisms from the soil domain with seldom physical conditions trigger the production of unique metabolites.

* Corresponding author.
** Corresponding author.
*E-mail addresses:* meghubhat09@gmail.com (M.P. Bhat), rmuthuraj20@gmail.com (M. Rudrappa), anilh5157@gmail.com (A. Hugar), poojagambhire123@gmail.com (P.V. Gunagambhire), sraju@ksu.edu.sa (R. Suresh Kumar), sreenivasankud@gmail.com (S. Nayaka), almansor@ksu.edu.sa (A.I. Almansour), pkarthikjaya@gmail.com (K. Perumal).

https://doi.org/10.1016/j.heliyon.2023.e21461
Received 30 July 2023; Received in revised form 25 September 2023; Accepted 21 October 2023
Available online 31 October 2023

**Abbreviations**

| | |
|---|---|
| % | : Percentage |
| ± | : Plus or minus |
| °C | : Degree Celsius |
| µ | : Micron(s) |
| µg | : Microgram |
| µg/mL | Microgram/milliliter |
| µL | : Micro liter |
| µM | : Micro molar |
| BLAST | Basic Local Alignment Search Tool |
| bp | : Base Pair |
| cm | : Centimeter |
| $CO_2$ | Carbon dioxide |
| DMSO | Dimethyl sulfoxide |
| DNA | Deoxyribonucleic acid |
| ELISA | Enzyme-Linked Immunosorbent Assay |
| et al | Others |
| FITC | Fluorescein Isothiocyanate |
| FTIR | Fourier Transform Infrared Spectroscopy |
| g | Gram(s) |
| GC-MS | Gas Chromatography-Mass Spectrometry |
| h | Hour(s) |
| *i.e.* | That is |
| IR | Infrared Radiation |
| L | Liter |
| *m/z* | Mass-to-Charge Ratio |
| MDR | Multiple Drug Resistant |
| MEGA | Molecular Evolutionary Genetic Analysis |
| mg | : Milligram |
| min | : Minute(s) |
| mM | : Milli molar |
| mm | : Millimeter |
| Mol. wt | Molecular weight |
| MS | : Mass spectra |
| MTT | 3-(4,5-dimethylthiazol-2-yl)-2,5-diphenyltetrazolium bromide |
| NCBI | National Center for Biotechnology Information |
| NCCS | National Centre for Cell Science |
| NIST | National Institute of Standards and Technology |
| OD | : Optical Density |
| PBS | Phosphate Buffer Saline |
| PDA | Potato Dextrose Agar |
| pH | : Potential of Hydrogen |
| PI | : Propidium Iodide |
| Rf | : Retardation factor |
| RNA | Ribonucleic acid |
| rRNA | ribosomal Ribonucleic Acid |
| SEM | Scanning Electron Microscope |
| Sl. No | Serial number |
| sp. | Species |
| Std | Standard |
| TLC | Thin Layer Chromatography |
| UV | Ultraviolet |
| UV–Vis | Ultraviolet–visible |
| v/v | Volume per Volume |
| viz. | Namely |

Among these microorganisms, fungi remain the persistent sources of essential natural products with various biological and industrial applications [4]. Naturally occurring products play a requisite part in exploring new drugs, and biologically important molecules obtained from natural entities account for around 50 % of the clinical drugs used for biomedical purposes [5,6].

The increased resistance towards clinical drugs among infectious microbes in the recent decade has instigated excessive drug usage that contributes to polluting the environment [7,8]. Fungi are the producers of several valuable secondary metabolites belonging to different chemical classes, such as alkaloids, steroids, and terpenes, among others; many life-saving drugs like penicillin, griseofulvin, cephalosporin, and β-lactams have been aiding the battle against disease-causing microorganisms [9,10].

The world population is enduring a significant challenge from infections, and new opportunistic pathogens that are surfacing to cause life-threatening infections worldwide [11,12]. Recently, the occurrence of yeast and frequent fungal infections has become the reason for increased mortality in immune-compromised individuals. Candidiasis is one of the most medically essential diseases worldwide whereby the most persistent is invasive candidiasis, followed by oral and dermal candidiasis of opportunistic yeast infections [13,14]. The constant and repeated usage of present-day antifungal drugs resulted in the virulent strain gaining resistance to particular drugs [15,16].

According to WHO, cancer is the leading cause of death in 112 out of 183 countries, while human blood and lymphocyte-related cancer is one of the significant cancer incidences. Human leukaemia cases are linearly increasing due to lifestyle, food habits, and smoking, with 60,650 new cases and more than 24,000 deaths in recent years [17,18]. The currently used chemotherapeutic drugs have fallen the pecking order due to their toxicity and side effects thereby new biological agents produced by fungi could be the replacement because of their non-toxicity and availability from nature [19,20].

Fungi inhabiting different habitats are widely inspected consistently because of their complex macromolecules with divergent structures and unique biochemical properties [21]. Several newly isolated biologically active compounds having important biological properties such as antioxidant, antimicrobial, insecticidal, anticancer, and antiviral have been extracted from fungi [22]. Many fungi-derived bio-control agents are ubiquitous such that they need to have effortless handling for mass production thereby it is feasible to control plant and human diseases. Therefore, bio-prospecting of fungal antagonists is necessary regarding the experimental success of bio-control agents [23,24].

*Talaromyces* is an important fungal genus because of its ubiquitous distribution comprising habitats like soil, marine, sponges, plants, and even foods. Few species among the genus are well-known producers of enzymes applicable in synthesizing saccharides, related biological macromolecules, and metabolites in biological control [25,26]. The *Talaromyces* species produce secondary metabolites in various chemical classes, such as azaphilone and isocoumarin derivatives, xanthones, sesquiterpenes, and benzofurans. The divergent biological activities, including antioxidant, antimicrobial, anti-tumour, and antiviral of bioactive compounds from *Talaromyces* species, make them suitable for bio-control purposes [27,28]. Squalene belongs to the terpenoid family which has an isoprenoid structure and is a natural lipid known to be a precursor for sterols, hormones, and vitamin synthesis. Squalene is helpful in cholesterol control and acts as an antioxidant, moisturizer, detoxifying and anticancer agent in cosmetics and biomedical fields [29,30].

Therefore, the present study focuses on producing biologically critical secondary metabolites from *Talaromyces pinophilus* CJ15 (CJ15) and evaluating their *in-vitro* biological activities that could aid in battling infections and blood cancer in humans.

## 2. Materials and methods

### 2.1. Soil sampling and collection of materials

Soil samples from different areas of forests in Dandeli, Karnataka, India, were dug out from about 4-inch depth from surface soil, assembled in sterilized numbered zip lock covers before being brought to the laboratory, and kept at room temperature until further study.

Pathogenic bacterial strains such as *Bacillus subtilis* (MTCC6633), *Shigella flexneri* (MTCC1457), *Staphylococcus aureus* (MTCC6908), and *Escherichia coli* (MTCC40), yeast strains such as *Candida albicans* (MTCC227), *Candida tropicalis* (MTCC1406), *Candida haemulonii* (MTCC1966), and *Candida glabrata* (MTCC3019) were obtained from Institute of Microbial Technology (IMTECH), Chandigarh, India. The fungal pathogens were procured from the Department of Plant Pathology, University of Agricultural Sciences, Dharwad. Hi-media laboratories in Mumbai, India provided all the necessary chemicals and reagents.

### 2.2. Fungal isolation from soil

About 1 g of each soil sample was dissolved in 10 ml distilled water to prepare stock and for $10^{-1}$ to $10^{-5}$ dilutions from the stock. Later, 100 μl suspension from each dilution was poured into Petri plates containing potato dextrose agar (PDA) media and followed by incubation for 7 days at room temperature. The fungal isolates with dissimilar colony morphology were noted such that it could help to distinguish and select individual isolates for sub-culturing on PDA.

### 2.3. Selection of potent strain by antagonistic activity

The cross streak (perpendicular streak) technique evaluated the ability of fungal strains to inhibit fungal growth on PDA media by inoculating the isolate at the center of the plate in a straight line. The pathogenic fungal strains such as *Sclerotium rolfsii*, *Colletotrichum* sp., *Cercospora canescens*, *Aspergillus niger*, *Fusarium sambucinum*, *Fusarium oxysporum*, and *Alternaria alternata* were inoculated at both the sides of the isolate followed by 7 days incubation at room temperature. The selected isolate was inoculated into PDB to facilitate the

secondary metabolite mass production.

### 2.4. Identification of potent strain by morphology

The fungal isolates were examined under a light microscope after 7 days of growth with the help of bright field optics at the desired magnification. The fungal isolate's simple staining was done using cotton blue dye to observe morphological features.

The effective isolate was analyzed using scanning electron microscopy (SEM) to observe the mycelium's structure, morphology, and spore arrangement. The SEM instrument used was a JSM-IT500 from JEOL, Kyoto, Japan. Thereafter, cut into discs, the fungus' mycelia were preserved in 2.5 % glutaraldehyde at 4 °C for 2 h. The fungal mycelia were dehydrated in an escalating series of ethanol for 30 min each after being washed twice with 0.1 M phosphate buffer saline (PBS, pH 7.8) for 1 min. The dehydrated mycelia were then mounted on carbon stubs, dried in a critical point drier (CPD), and finally coated with gold sputtering before the images were captured.

### 2.5. Genetic identification by gene sequencing

The sequencing of the 18S rRNA gene was enabled at the molecular level for the identification of potent isolate. The 18S rRNA gene was purified using an exonuclease-I shrimp alkaline phosphatase (Exo-SAP) after the DNA was extracted using a spin column kit (HiMedia, India). To remove the culture medium, the culture was first centrifuged at 10,000 rpm using a Remi R–8C. The pellet obtained was then re-suspended in 250 μl of lysis solution and 20 μl of RNase A solution, and incubated at 25 °C for 2 min. Proteinase-K solution containing about 25 μl was added, incubated at 55 °C for 30 min, vortexed horizontally, and then incubated once more at 95 °C for 10 min. The homogenous lysate was once again centrifuged at 12000 rpm after which it was transferred to a Hi-Elute Miniprep spin column and 500 μl of prewash solution was added. The column was then centrifuged at 10,000 rpm for 1 min, during this period the supernatant was removed. The DNA has now been centrifuged for 1 min at 10,000 rpm to elute it. With the use of the forward (1391f) and reverse (EukBr) primers, the region of 18S rRNA was amplified. The PCR reaction mixture consisted of template DNA (1.0 μl), $Mg2^{+}$ free buffer 5 μl, 2.5 μM magnesium chloride (5 μl), deoxyribonucleotide triphosphates (dntps) 8 μl (2.5 μM each dATP, dTTP, dGTP, dCTP), primer 1 μl each (20 μM each), *Taq* DNA polymerase 0.5 μl (5.0 U/μl), and molecular grade water to make up the volume up to 50 μl (Applied Biosystems 2720, Thermal Cycler, USA). Later, a 1 % agarose gel electrophoresis was used to confirm the PCR products using a 1 kb DNA ladder as a reference. Before being deposited at Genbank, the obtained 18S rRNA gene sequence was performed nucleotide BLAST analysis. Later, the obtained gene sequence was aligned with CLUSTAL-X software to determine the isolate's molecular evolutionary relationship. MEGA 7.0 software was then used to create a neighbour-joining phylogenetic tree using similar sequences from related species.

### 2.6. Preparation of crude extract

The potent isolate was inoculated in a 1L Erlenmeyer flask containing potato dextrose broth to facilitate secondary metabolite mass production. After the mycelium's maximum growth, the mycelia mat was separated from the culture supernatant by filtration, and an equal volume of ethyl acetate (99.8 %, AR grade) solvent was used for the extraction of cell-free culture broth following liquid-liquid extraction.

### 2.7. Characterizations of crude extract

#### 2.7.1. Fourier transform infrared spectroscopy (FTIR) analysis

The FTIR analysis was conducted to record the presence of various biochemical functional groups in crude ethyl acetate extract (EAE). The pellet sample for the analysis was prepared as a thin disc by mixing potassium bromide (KBr) with a pinch (0.1 mg) of dried extract. The prepared thin disc was then put into the sample holder and scanned at a rate of 4 $cm^{-1}$ using an FTIR instrument (Nicolet 6700, Thermo Fisher Scientific, Waltham, Massachusetts, USA) in the range of 4000 to 400 $cm^{-1}$.

#### 2.7.2. Gas chromatography-mass spectrometry (GC-MS) analysis

Helium was used as a carrier gas in the ELITE-5MS column (30 m × 0.25 mm, 0.25μ thickness) to perform the GC-MS analysis, which was carried out using an Agilent QP 2010S quadrupole mass analyzer with an electron multiplier detector (Kyoto, Japan). The column temperature was first set at 60 °C and subsequently increased to 280 °C for 5 min. Using a split-less injection technique, 2 ml of extract was added to the capillary column and left for up to 48 min. To identify the compounds, the resulting spectra were compared with the NIST 11 and WILEY 8 library databases.

#### 2.7.3. Column based purification of bioactive fraction

The crude EAE from CJ15 was purified using normal phase column chromatography. A clean and dried glass column (1.8 × 70 cm) was filled with silica gel (mesh size 230–400) as a packing material and equilibrated with 100 % petroleum ether. About 0.5 g of CJ15 crude EAE was solvated in petroleum ether. The column was eluted successively with a petroleum ether-methanol gradient solvent system (100 % petroleum ether/0 % methanol to 0 % petroleum ether/100 % methanol, v/v), and a totally 05 fractions were collected [100:0, 75:25, 50:50, 25:75, and 0:100, petroleum ether: methanol (v/v)]. The bioactive fraction was selected based on primary screening for antibacterial activity.

### 2.8. Evaluation of antimicrobial activity

The agar well diffusion method determined the antimicrobial activity of bioactive fraction 1, i.e. 100:0, petroleum ether: methanol, (v/v) (bioactive fraction) from the potent isolate. The inhibition potential of the bioactive fraction was tested against pathogenic bacteria such as *Staphylococcus aureus*, *Shigella flexneri*, *Bacillus subtilis*, and *Escherichia coli*. The dried bioactive fraction was dissolved in dimethyl sulfoxide (DMSO) as the solvent was not/less reactive towards microbes compared to other organic solvents like petroleum ether, chloroform, and others. The pathogen suspensions (100 μl of $10^6$ McFarland) were swabbed using cotton swabs on nutrient agar (NA) plates and thereafter, 6 wells each of 6 mm were made, and different concentrations of dried bioactive fractions as 25, 50, 75, and 100 μl were poured into separate wells. About 25 μl of streptomycin was used as the positive control and the negative control was DMSO (25 μl). After incubation at 37 °C for 24 h, the growth-less clear zones formed around the well were taken as inhibition zones and measured in millimeters.

### 2.9. Selection and identification of bioactive compound

#### 2.9.1. TLC based bio-autography for selecting bioactive compound

The TLC analysis was conducted to select and obtain partially purified bioactive fraction acquired through the column purification technique which used pre-coated silica gel aluminium plates (TLC Silica gel, 60 RP-18 $F_{254}$, Merck, Germany). The dried bioactive fractions obtained from CJ15 were re-dissolved in 1.0 ml of ethyl acetate, and 10 μl of prepared solutions were spotted as separate samples. The plates were developed inside a TLC chamber containing the solvent system toluene: ethyl acetate: methanol: acetic acid (5:3:1:0.5 v/v). Further, the developed plates were visualized under UV light to observe the formation of bands. Later, 2 similar plates from CJ15 were selected, in which 1 plate was taken as the reference, and the other was used for bio-autography by agar overlay method.

#### 2.9.2. Identification of bioactive compound by mass spectrometry

In GC-MS analysis, the ELITE-5MS column (Agilent QP2010S, Shimadzu, Kyoto, Japan) was used along with helium carrier gas while the initial temperature of the instrument was kept at 60 °C and increased gradually to 280 °C for 5 min. The injection port temperature was fixed at 260 °C and a 1 ml/min flow. The sample was injected by employing the split-less method and utilizing the NIST 11 and WILEY 8 libraries thereby the obtained spectrum was compared to identify the bioactive compound from the potent isolate.

### 2.10. Evaluation of candidicidal activity

To investigate the candidicidal potential of CJ15-derived bioactive compound, the agar well diffusion method was performed by swabbing *Candida* species like *C. haemulonii*, *C. albicans*, *C. tropicalis*, and *C. glabrata* on NA plates. Later, 5 wells of 6 mm diameter were made, and 25, 50 and 100 μl of bioactive compound were poured into respective wells; about 50 μl of amphotericin B and DMSO were taken as positive and negative controls, respectively. The 24 h incubation was done at 37 °C such that the zones of inhibition were measured in millimeters and recorded for all the tested pathogens.

The growth curve patterns of *C. albicans*, *C. haemulonii*, *C. tropicalis*, and *C. glabrata* treated with CJ15-derived bioactive compound were analyzed by UV–Vis. spectrophotometer. For the analysis, 1 mg of the dried bioactive compound was solvated in 1 ml of 10 % DMSO and mixed with 10 ml of nutrient broth (NB), whereas another tube with 1 ml of 10 % DMSO and 10 ml of NB was taken as a control. The pathogen suspensions of $10^6$ McFarland were inoculated into both tubes and immediately, the initial (0 h) optical density (OD) was recorded at 550 nm using a UV spectrophotometer (UV-9600A, METASH Instruments, Shanghai, China). Finally, the fungi inoculated in tubes were allowed to grow at room temperature, and at every 4 h intervals, OD was measured up to 28 h to determine growth curve patterns.

### 2.11. Determination of cytotoxicity by cell viability (MTT) assay

The anticancer capacity of CJ15-derived bioactive compound was determined on the human peripheral blood cancer cell line. The human leukaemia (JURKAT) cells were obtained from NCCS, Pune, India, and subcultured on DMEM-high glucose (#AL111, Himedia) medium. Further, only the cells which were without the test drug were taken as the negative control while the cells treated with 12.5 μg/ml of doxorubicin (#PHR1624, Sigma) were taken as the positive control. The CJ15-derived bioactive compound with different concentrations ranging from 12.25 to 200 μg/ml was poured into the wells in a 96-well plate before incubating at 37 °C for 24 h in a humidified 5 % $CO_2$ atmosphere (Healforce, China). Later, 50 μl of MTT reagent (#4060 Himedia) was added after removing the spent medium and following 3 h incubation, 100 μl of DMSO (#PHR1309, Sigma) was added to solubilize the MTT reagent. Finally, an ELISA reader was used to read the absorbance at 570 nm and the dose-response curve was plotted to determine the $IC_{50}$ concentration.

### 2.12. Statistical analysis

The assays were conducted three times (n = 3) and the average of those three parallel investigations constituted each value. The result was then presented as the mean ± standard deviation (±SD) of triplicates using Prism GraphPad 8.0.0 statistical analysis software.

## 3. Results

### 3.1. Isolation and selection of potent isolate

Twenty fungal isolates were obtained by serial dilution of soil samples collected from Dandeli, Karnataka, and numbered from CJ1 to CJ20. They were then screened for antagonistic activity to select the potent isolate CJ15 that exhibited activity against fungal phytopathogens such as *Aspergillus niger*, *Cercospora canescens*, *Alternaria alternata*, *Sclerotium rolfsii*, *Colletotrichum* spp., and *Fusarium* spp. The maximum inhibitory activity was observed against *Cercospora* sp. followed by *Alternaria alternata* and *Fusarium sambucinum*, whereas the minor inhibitory activity was observed against *Sclerotium rolfsii* (Fig. 1A–C).

### 3.2. Identification of potent strain by morphology

The observations from microscopic images displayed the morphology of CJ15 which was nearly comparable to that of *Penicillium*, a filamentous fungus in which the colony of CJ15 was white during initial growth (vegetative), and a greenish-yellow colour was observed during the reproductive phase. The microscopic image of CJ15 displayed smooth, coloured and septate conidiophores with hyaline hyphae. The spores were round to ovoid, situated on long, wavy spore chains (Fig. 2A&B). The morphological details observed through SEM micrograph displayed the septate hyphae with metulae wherein the metulae have few to many phialids or sterigmata that carry numerous spores assembled end to end on wavy-natured spore chains. It was also noticed that the spores were numerous and somewhat round (Fig. 2C&D).

### 3.3. Genetic characterization of isolate by 16S rRNA gene sequencing

The 18S rRNA gene sequence of 1021 base pairs length was obtained from isolate CJ15, and the gene sequence was deposited to the NCBI database with an accession number OP071593. Thus, the 18S rRNA gene sequence of CJ15 was taken to the nucleotide blast program on the NCBI website, which disclosed 99.90 % sequence similarity with *Talaromyces pinophilus* strain Naj102019. Later, the 18S rRNA gene sequence of isolate CJ15 was selected to construct the molecular evolutionary phylogeny of CJ15 with similar types of sequences of closely related species. Thus, the constructed phylogenetic tree displayed lateral branching between *Talaromyces pinophilus* CJ15 and *Talaromyces pinophilus* strain Naj102019 (Accession number: MK500622), establishing the molecular evolutionary relationship as shown in Fig. 3.

### 3.4. Preparation of ethyl acetate crude extract

The isolate *Talaromyces pinophilus* CJ15 (CJ15) was inoculated in 1L PDB to enhance the mass productiveness of secondary metabolites. After the maximum growth of mycelium, the mycelia were separated from culture filtrate, and the supernatant was used to extract extracellular secondary metabolites by liquid-liquid extraction method using ethyl acetate.

### 3.5. Determination of functional groups by FTIR analysis of crude EAE

The FTIR vibrational spectrum of CJ15 crude ethyl acetate extract exhibited 08 vibrational peaks corresponding to different biomolecules from 2924 to 845 $cm^{-1}$ in the scanning range (Fig. 4). The strong peak at 2924 $cm^{-1}$ represented N–H stretching amines and the medium peak at 2853 $cm^{-1}$ corresponded to C–H stretching alkanes. The strong peak at 1746 related to C═O stretching esters, and the two medium peaks at 1621 and 1456 $cm^{-1}$ correlated to C═C stretching conjugated alkenes and C–H bending alkane, respectively. Similarly, the remaining two weak peaks at 1217 and 845 $cm^{-1}$ represented the presence of C–O stretching tertiary alcohol and C–Cl stretching halo compounds, respectively.

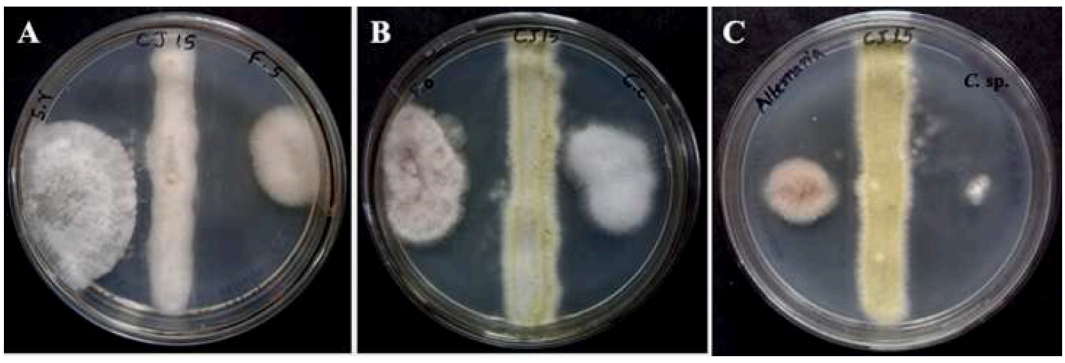


**Fig. 1.** Antagonistic activity of *Talaromyces pinophilus* CJ15; **A)** *Sclerotium rolfsii* and *Fusarium sambucinum*, **B)** *Fusarium oxysporum* and *Colletotrichum capsici*, and **C)** *Alternaria alternata* and *Cercospora* sp.

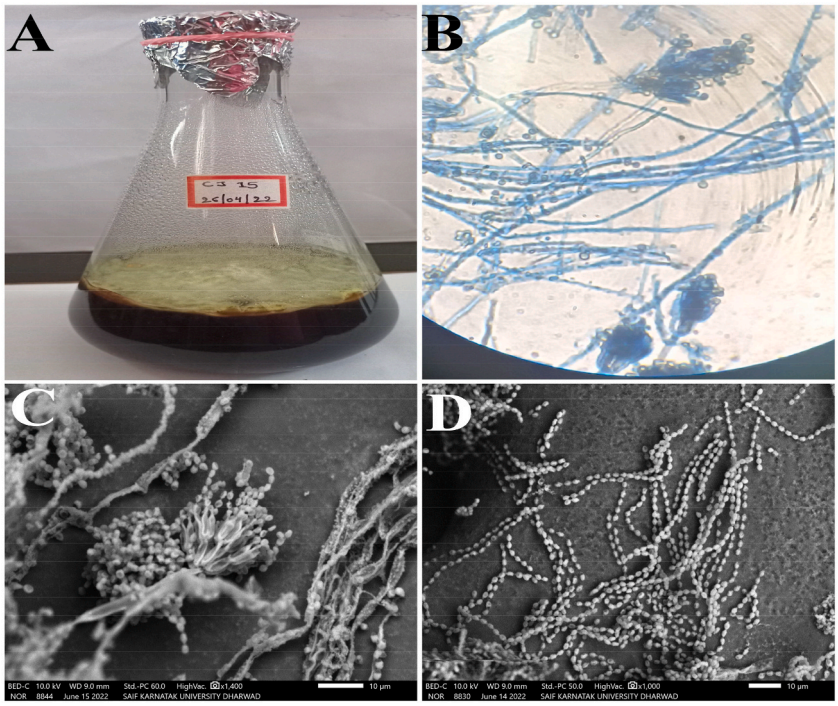


**Fig. 2.** Morphological features of *Talaromyces pinophilus* CJ15; **A)** Colony on PDB media, **B)** Microscopic image at 40× magnification, **C)** Morphology of CJ15 in SEM micrograph, and **D)** SEM image showing spore arrangement.

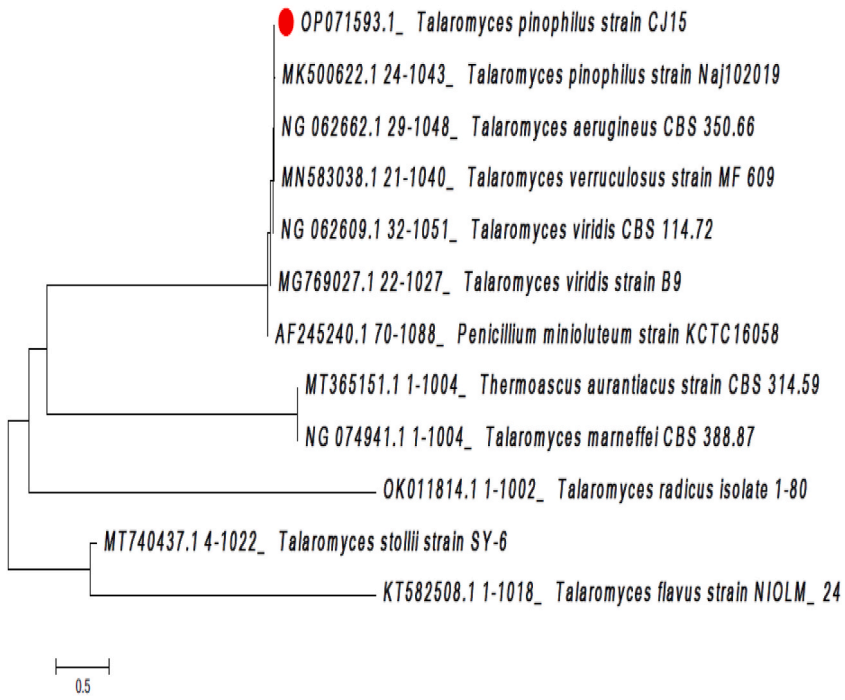


**Fig. 3.** Phylogenetic relationship of *Talaromyces pinophilus* CJ15 with closely related *Talaromyces* species.

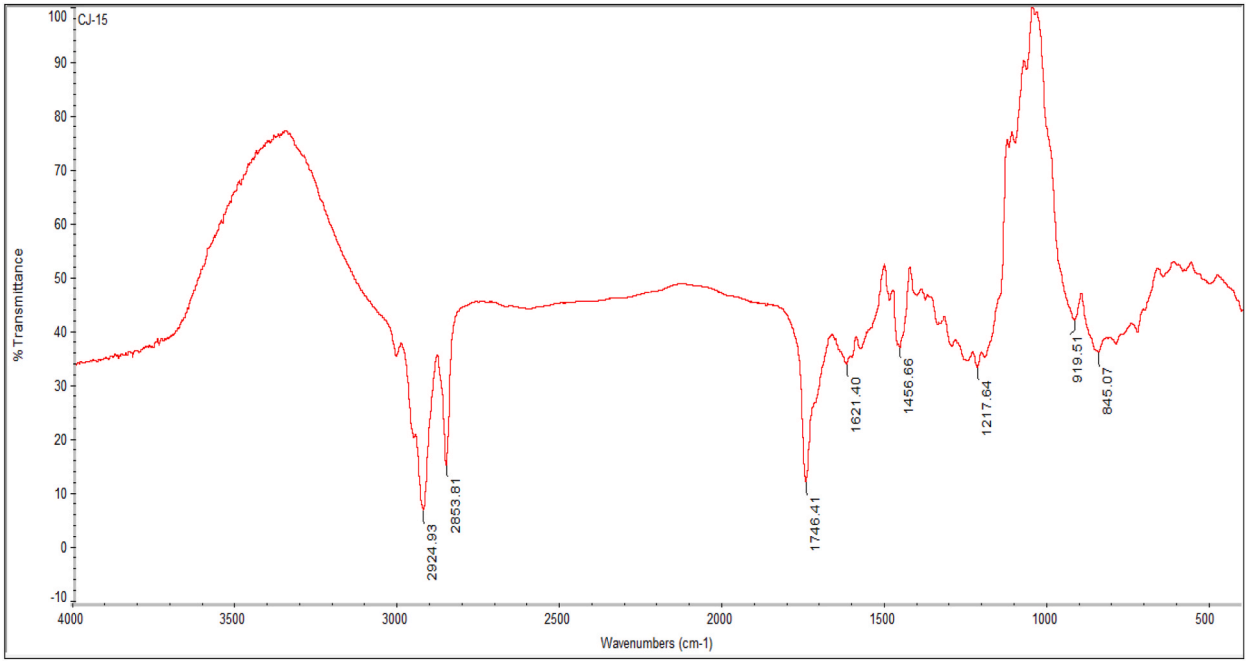


**Fig. 4.** FTIR spectrum of *Talaromyces pinophilus* CJ15 crude extract showing presence for various biological macromolecules.

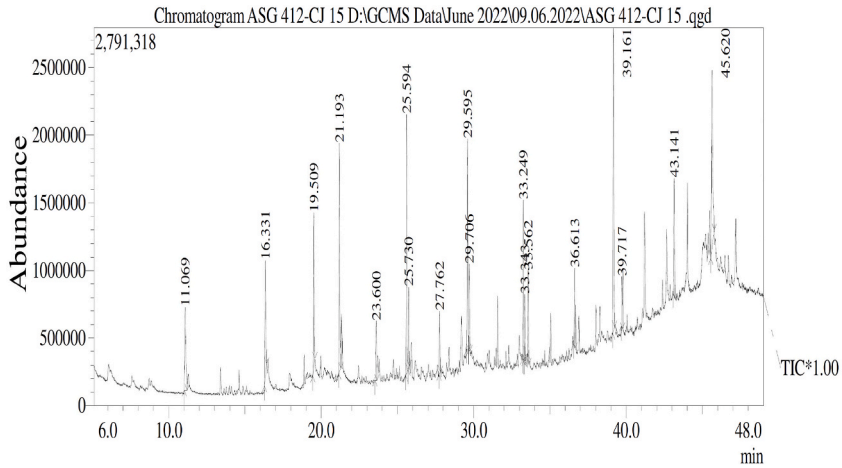


**Fig. 5.** GC-MS spectrum of *Talaromyces pinophilus* CJ15 crude ethyl acetate extract.

### *3.6. Compounds identification by GC-MS analysis of crude EAE*

The *Talaromyces pinophilus* CJ15 extract hinted at many biologically active molecules and compounds in GC-MS analysis (Fig. 5). The GC-MS spectrum was interpreted using the NIST 11 and WILEY 8 library databases. The GC-MS analysis of CJ15 revealed the presence of a total of 18 compounds, where a few compounds such as squalene, 2,4-ditert-butylphenol, E−15-heptadecenal, eicosane, and octadecane were recorded as bioactive. Among 18 compounds detected, about 11 were reported to have various biological activities, and the reports regarding the remaining 07 compounds' biological activities were not recorded yet. The compounds detected in the GC-MS spectrum are listed in Table 1.

### *3.7. Purification of crude EAE from CJ15*

The crude EAE from *Talaromyces pinophilus* CJ15 was purified by fractionation using gravity column chromatography to determine and obtain the bioactive fraction. Based on column chromatography, 05 fractions were obtained and dried in a rotary evaporator such that the antibacterial activity was done to select the most potent fraction (Fraction 1, 100 % petroleum ether/0 % methanol).

**Table 1**
Various compounds detected in GC-MS analysis of CJ15 crude ethyl acetate extract.

| RT | Area % | Compound name | Chemical formula | M.W. (g/mol) |
|---|---|---|---|---|
| 11.069 | 5.81 | Cyclopropane, nonyl- | $C_{12}H_{24}$ | 168.31 |
| 16.331 | 5.71 | 1-tetradecene | $C_{14}H_{28}$ | 196.37 |
| 19.509 | 6.74 | 2,4-ditert-Butylphenol | $C_{14}H_{22}O$ | 206.32 |
| 21.193 | 10.25 | 1-Hexadedcene | $C_{16}H_{32}$ | 224.42 |
| 23.600 | 2.74 | Heneicosane | $C_{21}H_{44}$ | 296.6 |
| 25.594 | 9.97 | E−15-Heptadecenal | $C_{17}H_{32}O$ | 252.4 |
| 25.730 | 2.87 | Octadecane | $C_{18}H_{38}$ | 254.49 |
| 27.762 | 2.15 | Nonadecane | $C_{19}H_{40}$ | 268.5 |
| 29.592 | 7.69 | E−14-Hexadecenal | $C_{16}H_{30}O$ | 238.41 |
| 29.706 | 2.89 | Iron, Tricarbonyl[Pheyl-2-Pyridinylmethylene) Benzenamine-N,N'] | $C_{21}H_{14}FeN_2O_3$ | 398.2 |
| 33.249 | 4.75 | 1-Octadecene | $C_{18}H_{36}$ | 252.5 |
| 33.343 | 2.14 | Eicosane | $C_{20}H_{42}$ | 282.5 |
| 33.562 | 2.90 | Heptadecyl acetate | $C_{19}H_{38}O_2$ | 298.50 |
| 36.613 | 2.43 | Heptadecyl trifluroacetate | $C_{19}H_{35}F_3O_2$ | 352.47 |
| 39.161 | 11.41 | 1,2-Benzenedicarboxylic acid | $C_8H_6O_4$ | 166.13 |
| 39.717 | 1.95 | Cyclodecane,Octyl- | $C_{18}H_{36}$ | 252.5 |
| 43.141 | 4.44 | Squalene | $C_{30}H_{50}$ | 410.7 |
| 45.620 | 13.15 | 1H-2-Indenone, 2,4,4,6,7,7a-hexahydro-3-(1-methylethyl)-7a-methyl | $C_{13}H_{20}O$ | 192.30 |

### 3.8. Antibacterial activity of CJ15 bioactive fraction

*Talaromyces pinophilus* CJ15, the extracted bioactive fraction was taken for antibacterial activity and concentrations such as 25, 50, 75, and 100 µl were loaded into separate wells. The bioactive fraction's potential was tested against Gram-positive and Gram-negative bacteria (Fig. 6A–D). It was observed that the highest inhibitory activity was shown against *Shigella flexneri* with 15, 18, 20, and 24 mm inhibition zones at concentrations of 25, 50, 75, 100 µl, respectively wherein *Staphylococcus aureus* was the most resistant among the pathogens, which showed lesser zones of inhibition of 08, 11, 12, and 16 mm for the respective 25, 50, 75, 100 µl concentrations of the bioactive fraction. The CJ15 extracted bioactive fraction exhibited moderate activity against the remaining pathogens as shown in Fig. 6E.

### 3.9. Selection and identification of bioactive compound

The selected fraction was further purified by TLC and bio-autography analysis. In TLC, the mobile phase consisted of toluene: ethyl acetate: methanol: acetic acid in the ratios of 5:3:1:0.5 by volume to separate pure compounds; a total of 04 spots were observed in the TLC plate under UV light (Fig. 7A).

The TLC plate was then used for bio-autography to select the bioactive compound by testing against *C. glabrata*. The band located at an $R_f$ value of 0.55 exhibited the activity by forming a clear area around the spot by inhibiting the growth of *C. glabrata* (Fig. 7B). Therefore, the bands at the $R_f$ value 0.55 from subsequent TLC plates were scraped, dissolved in petroleum ether and collected the dried compound for mass spectrum analysis. The GC-MS analysis of *Talaromyces pinophilus* CJ15 extracted compound confirmed the presence of squalene in the fragmentation mass spectrum with 69.05 base *m/z* value for molecular weight of 410.718 g/mol (Fig. 8), having the molecular formula $C_{30}H_{50}$.

### 3.10. Candidicidal activity of squalene

The agar well diffusion assay displayed the potential of squalene from CJ15 to inhibit the growth of pathogenic yeast strains such as *C. haemulonii*, *C. albicans*, *C. tropicalis*, and *C. glabrata* with increased activity with increasing volume (Fig. 9A–D). Amidst the tested yeast pathogens, *Candida albicans* was the most sensitive with 14, 16, and 18 mm zones of inhibition for the respective 25, 50, and 100 µl of squalene compared to 21 mm recorded for the positive control. The squalene exhibited moderate activity against *C. glabrata* and *C. tropicalis* with 17 and 16 mm at 100 µl, respectively such that *C. haemulonii* was the least sensitive with 10, 13, and 14 mm zones of inhibition for the respective 25, 50, and 100 µl of squalene treatments. The concentration-dependent activity of CJ15-derived squalene is represented in Fig. 9E.

The growth curve assay indicated the potential of squalene from CJ15 to inhibit the optimum growth of 04 *Candida* species by delaying the log phase in treated samples. In the control tubes, the turbidity was higher due to faster-growing yeast cells and cell debris, whereas, in the squalene-treated tubes, the turbidity was less because of the slow-growing rate throughout the observational period. The turbidity, in turn, played a vital role in determining growth curve patterns of tested *Candida* species in the control tubes whereby the linearly increasing optical density in the span of 28 h at 4 h intervals represented the standard sigmoid curve of growth of an organism. In contrast, the growth curve pattern of all 04 *Candida* species in the treated tubes did not represent the standard sigmoid curve because the shifting of the lag phase of the growth to the right side indicated delayed exponential growth. The results suggested the potential of squalene extracted from CJ15 to delay the adaptation period of all tested *Candida* species for exponential growth by almost 8 h than that of the control tube (Fig. 10A&B).

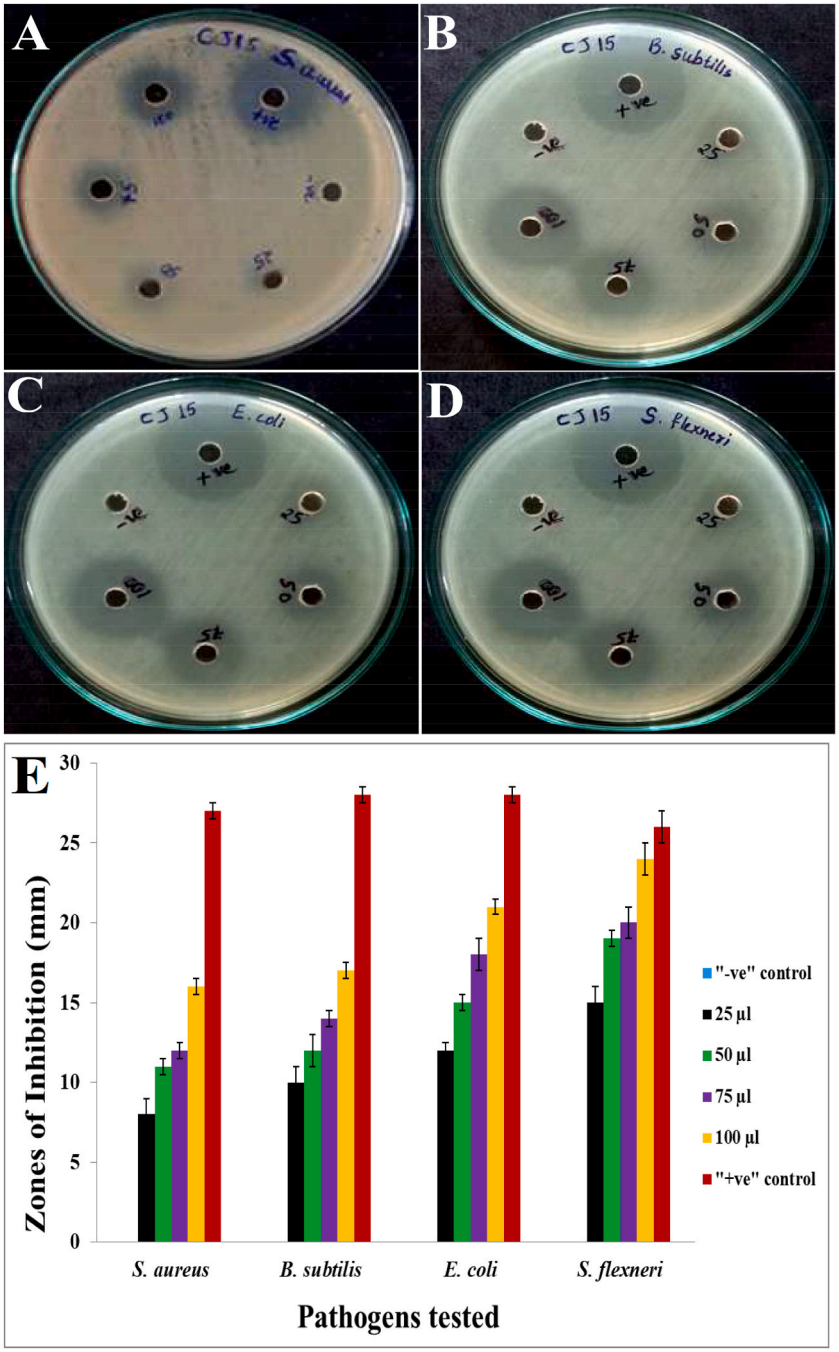


**Fig. 6.** Antibacterial activity of *Talaromyces pinophilus* CJ15 bioactive fraction against pathogens; **A)** *S. aureus*, **B)** *B. subtilis*, **C)** *E. coli*, and **D)** *S. flexneri*, and **E)** Graph showing concentration-dependent antibacterial activity of CJ15 bioactive fraction.

### *3.11. Cytotoxicity of squalene on JURKAT cells by cell viability (MTT) assay*

The cytotoxicity of *Talaromyces pinophilus* CJ15-derived squalene was evaluated on the JURKAT cell line and compared with untreated cells and the cells treated with standard drug doxorubicin (3 µM/ml). The morphological changes, including deformed cells, cell wall rupture, and outflow of the cytoplasmic matrix, were recorded using an inverted biological microscope at the magnification of 10X (100 µm), as shown in Fig. 11A–G. The results obtained by MTT assay in the JURKAT cell line exposed deformed cells when treated from 12.5 to 200 µg/ml concentrations for 24 h thereby the results exhibited decreased cell viability with increased concentration against the JURKAT cell line. The recorded cell viabilities were 63.10 %, 52.66 %, 39.12 %, 21.11 %, and 7.49 %, respectively, at 12.5,

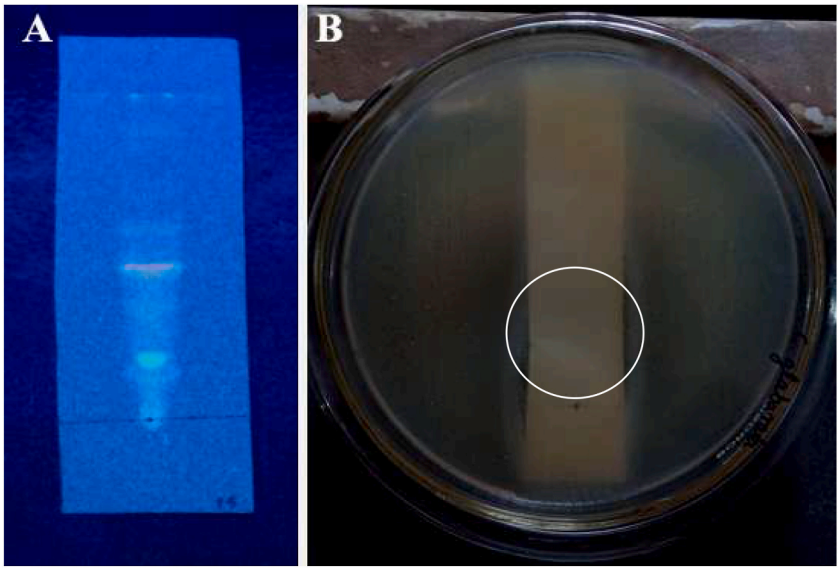


**Fig. 7.** TLC based bio-autography of *Talaromyces pinophilus* CJ15 derived bioactive fraction; **A)** TLC plate showing band pattern, and **B)** Bio-autography plate showing activity of fraction 1 against *C. glabrata*.

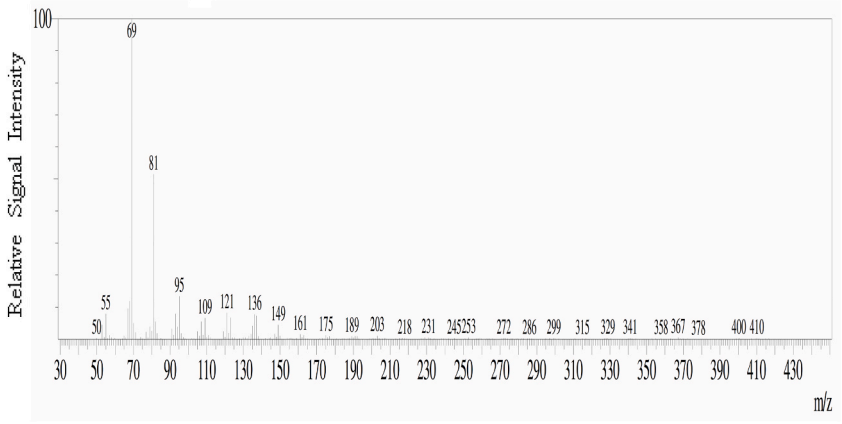


**Fig. 8.** Fragmentation mass spectrum of squalene derived from *Talaromyces pinophilus* CJ15.

25, 50, 100, and 200 μg/ml concentrations of squalene. The MTT assay showed that *Talaromyces pinophilus* CJ15-derived squalene exhibited concentration-dependent cytotoxicity against the JURKAT cell line, and it showed significant cytotoxicity on human acute leukaemia cells *in-vitro* by reducing the % cell viability with an increase in treatment concentrations (Fig. 11H). The $IC_{50}$ of CJ15-derived squalene was determined to be 26.22 μg/ml against the JURKAT cell line.

## 4. Discussion

The deep forest is one of the peculiar habitats for microbes, especially fungi, because of its nutrient-rich organic matter, optimal humidity, and less human activities. The earlier investigations on fungi isolated from forest soil suggested that the deep forest offers optimal growth parameters and induces unique secondary metabolite production when exposed to extreme conditions [17,31]. The primary screening by dual culture showed the increased potential of CJ15 for antagonistic activity such that the potential of inhibiting pathogenic fungal growth may be due to bioactive secondary metabolites released by the antagonistic isolate. The studies regarding the inhibitory activity of swamp forest actinomycete *Streptomyces* sp. KF15 suggested that the microbes produce bioactive secondary metabolites under stress, and the secreted bioactive metabolites disseminate through the culture medium thereby preventing the pathogen from growing further [32,33].

The morphological details such as branched hyphae, septate and filamentous mycelium buttress numerous round-shaped spores at the top end of the vesicle were observed. The literature describing the genus *Talaromyces* also reported effusively branched hyphae and multinucleated hyaline mycelium with septa wherein the mycelium bears numerous conidial spores arranged in chains. The conidial

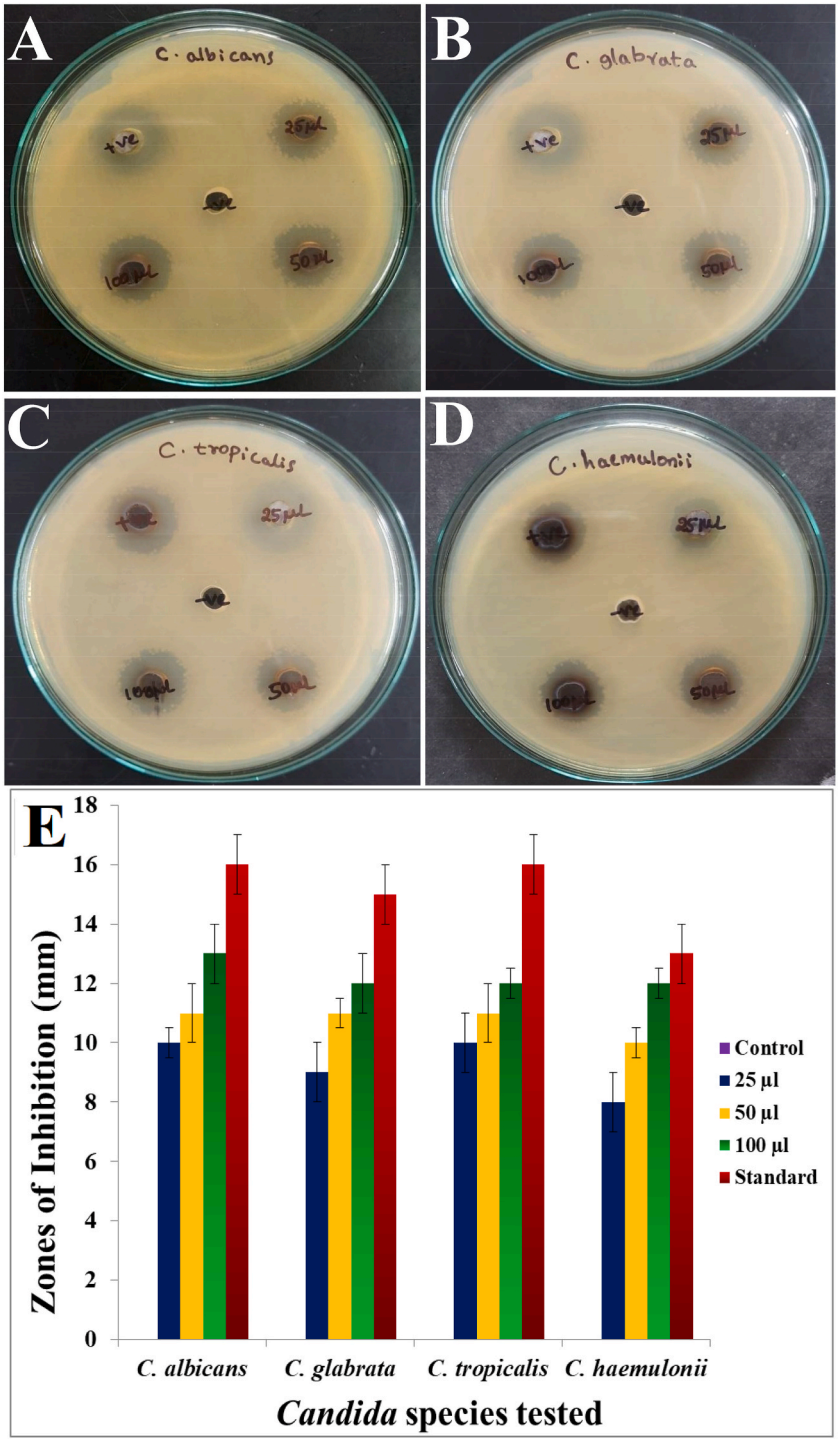


**Fig. 9.** Candidicidal activity of *Talaromyces pinophilus* CJ15 derived squalene against selected *Candida* species; **A)** *C. albicans*, **B)** *C. glabrata*, **C)** *C. tropicalis*, **D)** *C. haemulonii*, and **E)** Graph showing concentration-dependent candidicidal activity of squalene.

spores were described as ornamented, mostly globose, and unicellular [34]. Based on the 18S rRNA gene sequencing, the isolate CJ15 was identified as the *Talaromyces pinophilus* strain, and the reconstructed evolutionary phylogenetic tree established the relationship with *Talaromyces pinophilus* strain Naj102019 by forming a lateral branch. These results were supported by the previous reports, where the isolates DYM25 and ABRF2 were identified as *Talaromyces purpureogenus* strains based on 18S rRNA gene sequence followed by the analysis of the constructed molecular phylogenetic tree [35,36].

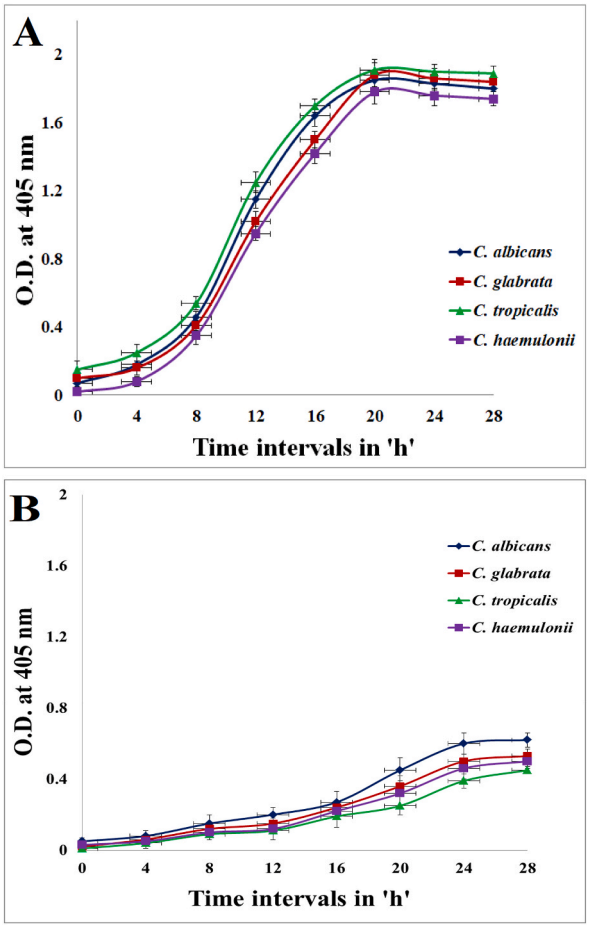


**Fig. 10.** Growth curve assay against *Candida* species; **A)** Control sample, and **B)** Sample treated with squalene.

The FTIR spectrum of CJ15 extract revealed the existence of diverse secondary metabolites belonging to various chemical classes. The previous study involving FTIR analysis of *Talaromyces* purpureogenus reported the presence of absorption bands representing different functional groups such as alkanes, aldehydes, ketones, alcohols, nitro compounds, ethers, phthalates, esters, and phenols [36]. The compounds such as squalene, E−15-Heptadecenal, 2,4-ditert-butylphenol, eicosane, and octadecane detected in the GC-MS of extract stipulated the combined action of metabolites in the extract. They hinted at possible antimicrobial and anticancer agents. Similarly, in the previous investigations, the secondary metabolites with biological activities were detected and identified through GC-MS analysis. The reports stated that compounds like eicosane, heneicosane, nonadecane, tetradecane, dibuty phthalate, 2, 4-di-*tert*-butylphenol, oleic acid, n-hexadecanoic acid, and many more had different bioactivities such as antibiotic, anti-inflammatory, antifungal, anticancer, and anti-viral that could be beneficial for battling severe diseases [37,38].

The *Talaromyces pinophilus* CJ15-derived bioactive fraction exhibited increased antimicrobial activity against *Shigella flexneri*, a Gram-negative bacterium wherein the bioactive fraction could prevent the growth of tested pathogens at varying capacities. The previous investigations on the antimicrobial activity of *Talaromyces* species suggested that among different solvents used, ethyl acetate extract was the one that displayed the highest activity when compared with the crude extracts of other organic solvents [39,40]. Another study reported that the difference in inhibition activity between Gram-positive and Gram-negative bacteria was due to the dissimilarities of cell wall composition and cell membrane permeability [41]. In other reports, the results suggested the wide range of antimicrobial activity displayed by ethyl acetate crude extract, in which the highest activity was noted against *Proteus mirabilis* by forming 15–23 mm inhibition zones. They also suggested the concentration-dependent activity of crude extract [42,43]. The previous studies suggested the turbidimetry method as one of the easiest, most reliable and brisk methods for antimicrobial activities. They can effectively establish the comparison between the control and treated samples. The reports described the right-sided shift as correlated to a delayed lag phase with lower reproduction rates and germination rates of treated cells compared to control cells. These factors affected the exponential growth by preventing Candida species from gaining the required turbidity [13,44,45].

The CJ15-derived squalene illustrated concentration-dependent cytotoxic activity against the JURKAT cell line by inducing 92.51 % cell death at 200 μg/ml concentration. The $IC_{50}$ concentration as low as 26.22 μg/ml suggested an increased potential of CJ15-derived squalene to effectively prevent the JURKAT cancer cell growth. Similar observations were recorded in cytotoxicity studies

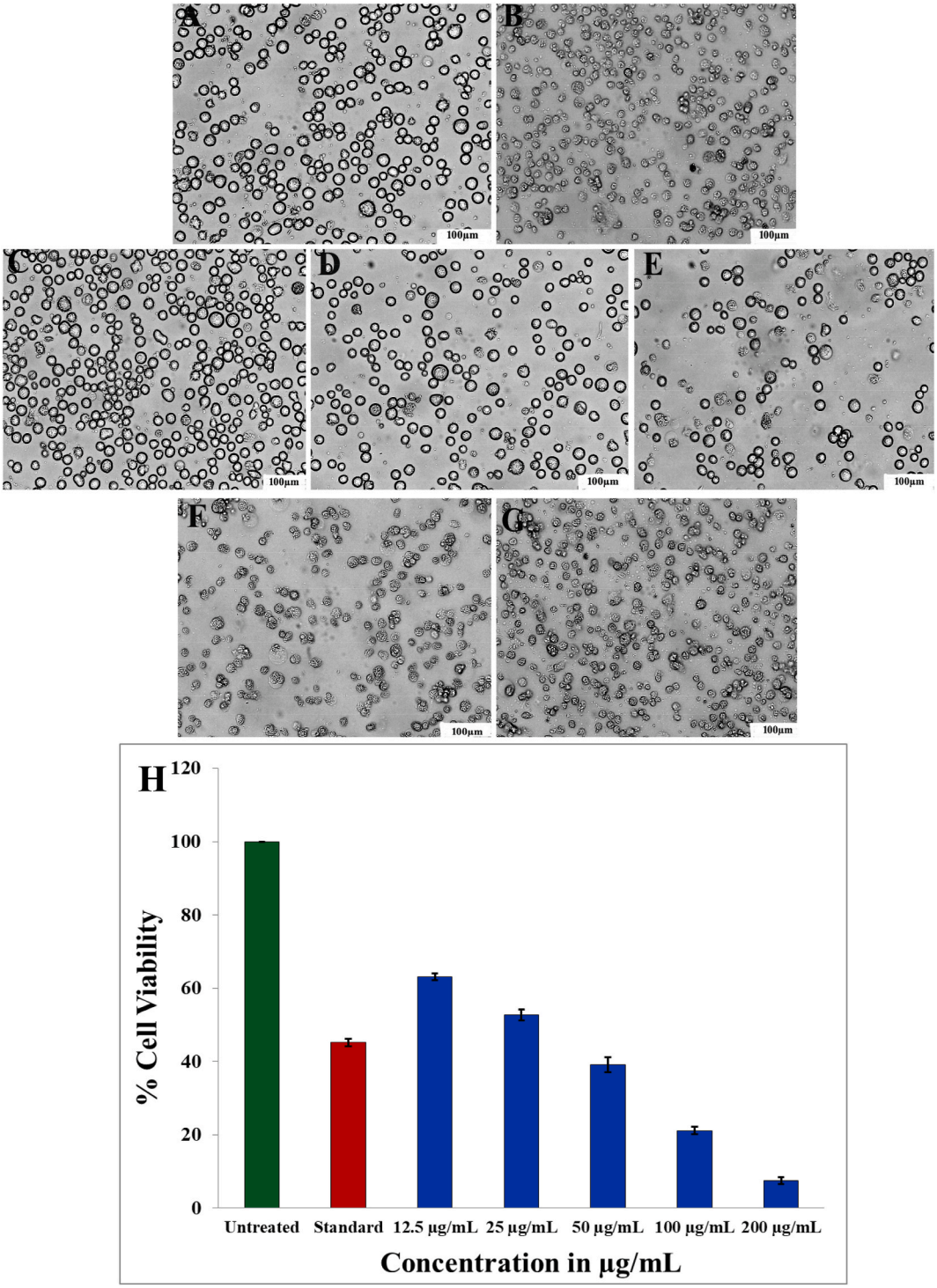


**Fig. 11.** Anticancer activity of *Talaromyces pinophilus* CJ15 extracted squalene on JURKAT cell line; **A)** Untreated cells, **B)** Std. doxorubicin treated cells, **C)** 12.5 µg/ml squalene treated cells, **D)** 25 µg/ml squalene treated cells, **E)** 50 µg/ml squalene treated cells, **F)** 100 µg/ml squalene treated cells, and **G)** 200 µg/ml squalene treated cells, and **H)** Graph showing dose-dependent activity of squalene against JURKAT cell line.

of *Talaromyces funiculosus*, *T. purpureogenus*, and *T. assiutensis* extracts against different human cancer cell lines, including HCT116, MCF7, HepG2, HeLa, A549, A-431, LN-229, and normal human embryonic kidney cell line HEK 293T. In their studies, fungal crude extracts revealed exceptionally higher tumour-suppressing activity in breast cancer (MCF-7), cervical cancer (HeLa), and human colon

cancer (HepG2) cells with $IC_{50}$ concentration of 100–200 μg/ml. The study reported significantly less or no cytotoxicity towards the normal human embryonic kidney cell line HEK 293T, indicating a less harmful effect of fungal extract [46–48]. Other studies reported the cytotoxic activity of squalene against KB/C152, HepG2, Hek293, and HUT-78/C185 cell lines with low $IC_{50}$ concentrations of 6.1–100 μg/ml [49,50].

Furthermore, squalene-treated cells displayed shrunken and distorted cells showing irregular margins and collapsed cell membranes. Cellular changes like ruptured cell walls, swollen cells, and mixed chromatins were reported in fungal bioactive compound-treated cancer cells [51]. Another study reported a large population of depleted necrotic cells with collapsed cell membranes and cells showing rough/lumpy cell and nuclear membranes in treated cancer cells [52].

## 5. Conclusions

The bio-prospecting of *Talaromyces pinophilus* CJ15 revealed its broad-spectrum antagonistic activity, and the FTIR and GC-MS analyses of crude extract illustrated several functional groups and bioactive compounds. The combined action of extract-derived biomolecules inhibited the growth of both Gram-positive and Gram-negative bacteria at different concentrations. The growth curve assay depicted a significant delay in the exponential growth of all the treated *Candida* species, suggesting the increased potential of CJ15-derived squalene. The anticancer activity displayed the potential of CJ15-derived squalene to inhibit the proliferation of JURKAT cells at a lower $IC_{50}$ concentration of 26.22 μg/ml and inflicted apoptosis-induced cell death *in-vitro*. Thus, our findings encourage researchers to explore the development of biomolecules derived from biological agents that could help battle infections and blood cancer in humans.

## Ethical approval

Not Applicable.

## Funding

This project was supported by the Researchers Supporting Project number (RSP2023R231), King Saud University, Riyadh, Saudi Arabia.

## Data availability statement

Data will be made available upon request. The 18S rRNA gene sequence of *Talaromyces pinophilus* CJ15 has been deposited to GenBank in the NCBI database with accession number: OP071593.

## CRediT authorship contribution statement

**Meghashyama Prabhakara Bhat:** Methodology, Writing – original draft, Writing – review & editing, Data curation. **Muthuraj Rudrappa:** Data curation, Methodology. **Anil Hugar:** Validation, Writing – review & editing. **Pooja Vidyasagar Gunagambhire:** Validation, Writing – review & editing. **Suresh Kumar Raju:** Conceptualization, Investigation, Supervision. **Sreenivasa Nayaka:** Conceptualization, Investigation, Supervision. **Abdulrahman I. Almansour:** Funding acquisition, Investigation. **Karthikeyan Perumal:** Software, Visualization.

## Declaration of competing interest

The authors declare that they have no known competing financial interests or personal relationships that could have appeared to influence the work reported in this paper.

## Acknowledgments

The authors would like to thank the P.G. Department of Studies in Botany, Karnatak University, Dharwad for rendering laboratory facility and Sophisticated Analytical Instrumentation Facility (SAIF, USIC), Karnatak University, Dharwad for providing necessary instrumentation facilities.

## References

[1] D. Zhang, Y. Tang, J. Yang, Y. Gao, C. Ma, L. Che, J. Wang, J. Wu, J. Zheng, De novo design of allochroic zwitterions, Mater. Today 60 (2022) 17, https://doi.org/10.1016/j.mattod.2022.09.001.

[2] D. Zhang, Y. Tang, K. Zhang, Y. Xue, S.Y. Zheng, B. Wu, J. Zheng, Multiscale bilayer hydrogels enabled by macrophase separation, Matter 6 (2023) 1484, https://doi.org/10.1016/j.matt.2023.02.011.

[3] D. Zhang, Y. Tang, C. Zhang, F.N.U. Huhe, B. Wu, X. Gong, S.S.C. Chuang, J. Zheng, Formulating zwitterionic, responsive polymers for designing smart soils, Small 18 (2022), 2203899, https://doi.org/10.1002/smll.202203899.

[4] N.E. Awad, H.A. Kassem, M.A. Hamed, A.M. El-Feky, M.A.A. Elnaggar, K. Mahmoud, M.A. Ali, Isolation and characterization of the bioactive metabolites from the soil fungus *Trichoderma viride*, Mycol. 9 (2018) 70, https://doi.org/10.1080/21501203.2017.1423126.

[5] R. Conrado, T.C. Gomes, G.S.C. Roque, A.O. De Souza, Overview of bioactive fungal secondary metabolites: cytotoxic and antimicrobial compounds, Antibiot 11 (2022) 1604, https://doi.org/10.3390/antibiotics11111604.

[6] H. Abdel-Hady, M.T.A. Abdel-Wareth, E.A. El-Wakil, E.A. Helmy, Identification and evaluation of antimicrobial and cytotoxic activities of *Penicillium islandicum* and *Aspergillus tamarii* ethyl acetate extracts, World J. Pharm. Pharmaceut. Sci. 5 (2016) 2021, https://doi.org/10.20959/wjpps20169-7674.

[7] N. Kaur, D.S. Arora, Prospecting the antimicrobial and antibiofilm potential of *Chaetomium globosum* an endophytic fungus from *Moringa oleifera*, Amb. Express 10 (2020) 206, https://doi.org/10.1186/s13568-020-01143-y.

[8] M. Vasundhara, M.S. Reddy, A. Kumar, Secondary metabolites from endophytic fungi and their biological activities, in: New and Future Developments in Microbial Biotechnology and Bioengineering, Elsevier B.V., Amsterdam, 2019, pp. 237–252, https://doi.org/10.1016/B978-0-444-63504-4.00018-9.

[9] A. Baazeem, A. Almanea, P. Manikandan, M. Alorabi, P. Vijayaraghavan, A. Abdel-Hadi, Vitro antibacterial, antifungal, nematocidal and growth promoting activities of *Trichoderma hamatum* FB10 and its secondary metabolites, J. Fungi 7 (2021) 331, https://doi.org/10.3390/jof7050331.

[10] W. Chen, C. Chen, J. Long, S. Lan, X. Lin, S. Liao, B. Yang, X. Zhou, J. Wang, Y. Liu, Bioactive secondary metabolites from the deep-sea derived fungus *Aspergillus* sp. SCSIO 41029, J. Antibiot. (2020), https://doi.org/10.1038/s41429-020-00378-y.

[11] J.R. Kohler, A. Casadevall, J. Perfect, The spectrum of fungi that infects humans, Cold Spring Harb. Perspect. Med. 5 (2015) a019273, https://doi.org/10.1101/cshperspect.a019273.

[12] G. Janbon, J. Quintin, F. Lanternier, C. d'Enfert, Studying fungal pathogens of humans and fungal infections: fungal diversity and diversity of approaches, Gene Immun. 20 (2019) 403, https://doi.org/10.1038/s41435-019-0071-2.

[13] M. Nordin, W.H.A.W. Harun, F.A. Razak, Antifungal susceptibility and growth inhibitory response of oral *Candida* species to *Brucea javanica* Linn. extract, BMC Complem.Altern. Med. 13 (2013) 342. http://www.biomedcentral.com/1472-6882/13/342.

[14] G. Pinilla, Y.T. Coronado, G. Chaves, L. Munoz, J. Navarrete, L.M. Salazar, C.P. Taborda, J.E. Muno, In vitro antifungal activity of LL-37 analogue peptides against *Candida* spp, J. Fungi 8 (2022) 1173, https://doi.org/10.3390/jof8111173.

[15] P.G. Deutsch, J. Whittaker, S. Prasad, Invasive and non-invasive fungal rhino-sinusitis -a review and update of the evidence, Medicina 55 (2019) 319, https://doi.org/10.3390/medicina55070319.

[16] A. Sasi, E.B. Raj, T. Soundarya, K. Marikani, S. Dhanasekaran, N. Al-Dayan, A.A. Mohammed, Exploring antifungal activities of acetone extract of selected Indian medicinal plants against human dermal fungal pathogens, Saudi J. Biol. Sci. 28 (2021) 2180, https://doi.org/10.1016/j.sjbs.2021.01.046.

[17] N. Kaur, D.S. Arora, N. Kalia, M. Kaur, Antibiofilm, antiproliferative, antioxidant and antimutagenic activities of an endophytic fungus *Aspergillus fumigatus* from *Moringa oleifera*, Mol. Biol. Rep. 47 (2020) 2901, https://doi.org/10.1007/s11033-020-05394-7.

[18] H. Sung, J. Ferlay, R.L. Siegel, M. Laversanne, I. Soerjomataram, A. Jemal, F. Bray, Global cancer statistics 2020: GLOBOCAN estimates of incidence and mortality worldwide for 36 cancers in 185 countries, CA Cancer J. Clin. 71 (2021) 209, https://doi.org/10.3322/caac.21660.

[19] R.L. Siegel, K.D. Miller, H.E. Fuchs, A. Jemal, Cancer statistics, 2022, Cancer J. Clin. 72 (2022) 7, https://doi.org/10.3322/caac.21708.

[20] A.K. Farha, A.M. Hatha, Bioprospecting potential and secondary metabolite profile of a novel sediment-derived fungus *Penicillium* sp. ArCSPf from continental slope of eastern Arabian sea, Mycol. 10 (2019) 109, https://doi.org/10.1080/21501203.2019.1572034.

[21] M.M. Qader, A.A. Hamed, S. Soldatou, M. Abdelraof, M.E. Elawady, A.S.I. Hassane, L. Belbahri, R. Ebel, M.E. Rateb, Antimicrobial and antibiofilm activities of the fungal metabolites isolated from the marine endophytes *Epicoccum nigrum* M13 and *Alternaria alternata* 13A, Mar. Drugs 19 (2021) 232, https://doi.org/10.3390/md19040232.

[22] E. Noman, M.M. Al-Shaibani, M.A. Bakhrebah, R. Almoheer, M. Al-Sahari, A. Al-Gheethi, R.M.S.R. Mohamed, Y.Q. Almulaiky, W.H. Abdulaal, Potential of anti-cancer activity of secondary metabolic products from marine fungi, J. Fungi 7 (2021) 436, https://doi.org/10.3390/jof7060436.

[23] J. Poveda, P. Baptista, Filamentous fungi as biocontrol agents in olive (*Olea europaea* L.) diseases: mycorrhizal and endophytic fungi, Crop Prot. 146 (2021), 105672, https://doi.org/10.1016/j.cropro.2021.105672.

[24] M. Tagawa, H. Tamaki, A. Manome, O. Koyama, Y. Kamagata, Isolation and characterization of antagonistic fungi against potato scab pathogens from potato field soils, FEMS Microbiol. Lett. 305 (2021) 136, https://doi.org/10.1111/j.1574-6968.2010.01928.x.

[25] L. Lei, L. Gong, M. Jin, R. Wang, R. Liu, J. Gao, M. Liu, L. Huang, G. Wang, D. Wang, Y. Deng, Research advances in the structures and biological activities of secondary metabolites from *Talaromyces*, Front. Microbiol. 13 (2022), 984801, https://doi.org/10.3389/fmicb.2022.984801.

[26] R. Nicoletti, A. Trincone, Bioactive compounds produced by strains of *Penicillium* and *Talaromyces* of marine origin, Mar. Drugs 14 (2016) 37. https://doi:10.3390/md14020037.

[27] M. Zhai, J. Li, C. Jiang, Y. Shi, D. Di, P. Crews, Q. Wu, The bioactive secondary metabolites from *Talaromyces* species, Nat. Prod. Bioprospect. 6 (2016) 1. https://doi:10.1007/s13659-015-0081-3.

[28] L. Feng, B. Zhang, H. Zhu, L. Pan, F. Cao, Bioactive metabolites from *Talaromyces purpureogenus*, an endophytic fungus from *Panax notoginseng*, Chem. Nat. Comp. (2020) 56. https://doi:10.1007/s10600-020-03206-9.

[29] J.M. Lou-Bonafonte, R. Martínez-Beamonte, T. Sanclemente, J.C. Surra, L.V. Herrera-Marcos, J. Sanchez-Marco, C. Arnal, J. Osada, Current insights into the biological action of squalene, Mol. Nutr. Food Res. 62 (2018) 1800136. https://doi:10.1002/mnfr.201800136.

[30] M.A. Lozano-Grande, S. Gorinstein, E. Espitia-Rangel, G. D'avila-Ortiz, A.L. Martinez-Ayala, Plant sources, extraction methods, and uses of squalene, Int. J. Agron. (2018), 1829160, https://doi.org/10.1155/2018/1829160.

[31] G.F. Bills, J.B. Gloer, Biologically active secondary metabolites from the fungi, Microbiol. Spectr. 4 (2016), https://doi.org/10.1128/microbiolspec.FUNK-0009-2016.

[32] M.P. Bhat, S. Nayaka, R.S. Kumar, A swamp forest *Streptomyces* sp. strain KF15 with broad spectrum antifungal activity against chilli pathogens exhibits anticancer activity on HeLa cells, Arch. Microbiol. 204 (2022) 540, https://doi.org/10.1007/s00203-022-03147-7.

[33] M.P. Bhat, S. Nayaka, Cave soil *Streptomyces* sp. strain YC69 antagonistic to chilli fungal pathogens exhibits in vitro anticancer activity against human cervical cancer cells, Appl. Biochem. Biotechnol. (2023), https://doi.org/10.1007/s12010-023-04388-y.

[34] C.J. Alexopoulos, C.W. Mims, Introductory Mycology, third ed., Wiley, New York, 1979, pp. 24–25.

[35] M. Luo, Y. Chen, J. He, X. Tang, X. Wu, C. Xu, Identification of a new *Talaromyces* strain DYM25 isolated from the Yap Trench as a biocontrol agent against *Fusarium* wilt of cucumber, Microbiol. Res. 251 (2021), 126841, https://doi.org/10.1016/j.micres.2021.126841.

[36] M.K. Sahu, K. Kaushik, A. Das, H. Jha, In vitro and in silico antioxidant and antiproliferative activity of rhizospheric fungus *Talaromyces purpureogenus* isolate-*ABRF2*, Bioresour. Bioprocess. 7 (2020) 14, https://doi.org/10.1186/s40643-020-00303-z.

[37] O.A. Adelusi, S. Gbashi, J.A. Adebiyi, R. Makhuvele, O.A. Adebo, A.O. Aasa, S. Targuma, G. Kah, P.B. Njobeh, Variability in metabolites produced by *Talaromyces pinophilus* SPJ22 cultured on different substrates, Fungal Biol. Biotechnol. 9 (2022) 15, https://doi.org/10.1186/s40694-022-00145-8.

[38] K.N. Dharshini, G. Jothi, N. Swarnakumari, L. Rajendra, Gas chromatography: mass spectrometry (GC-MS) analysis of biomolecules from *Talaromyces pinophilus*, Pharm. Innov. 10 (2021) 971.

[39] A. Singh, M. Kumar, R.K. Salar, Isolation of a novel antimicrobial compounds producing fungus *Aspergillus niger* MTCC 12676 and evaluation of its antimicrobial activity against selected pathogenic microorganisms, J. Pure Appl. Microbiol. 11 (2021) 1457, https://doi.org/10.22207/JPAM.11.3.29.

[40] F. Song, Y. Dong, S. Wei, X. Zhang, K. Zhang, X. Xu, New antibacterial secondary metabolites from a marine-derived *Talaromyces* sp. strain BTBU20213036, Antibiot 11 (2022) 222, https://doi.org/10.3390/antibiotics11020222.

[41] L.D. Witasari, K.W. Wahyu, B.J. Anugrahani, D.C. Kurniawan, A. Haryanto, D. Nandika, L. Karlinasari, A. Arinana, I. Batubara, D. Santoso, Y. Rachmayanti, D. Firmansyah, I.K. Sudiana, D.M. Hertanto, Antimicrobial activities of fungus comb extracts isolated from Indomalayan termite (*Macrotermes gilvus* Hagen) mound, Amb. Express 12 (2022) 14, https://doi.org/10.1186/s13568-022-01359-0.

[42] M. Thorati, J.K. Mishra, Antibacterial activity of crude extract from *Aspergillus niger* isolated from the stilt roots of *Rhizophora apiculata* along South Andaman coast, India, J. Pharmacogn. Phytochem. 6 (2017) 1635.

[43] M.P. Bhat, B. Chakraborty, S.K. Nagaraja, P.V. Gunagambhire, R.S. Kumar, S. Nayaka, A.I. Almansour, K. Perumal, *Aspergillus niger* CJ6 extract with antimicrobial potential promotes *in-vitro* cytotoxicity and induced apoptosis against MIA PaCa-2 cell line, Environ. Res. 229 (2023), 116008, https://doi.org/10.1016/j.envres.2023.116008.
[44] M.T. Blanco, C. Perez-Giraldo, J. Blanco, F.J. Moran, C. Hurtado, A.C. Gomez-Garcia, In vitro studies of activities of some antifungal agents against *Candida albicans* ATCC10231 by the turbidimetric method, Antimicrob. Agents Chemother. 36 (1992) 898, https://doi.org/10.1128/AAC.36.4.898.
[45] J. Meletiadis, D.T.A. Dorsthorst, P.E. Verweij, Use of turbidimetric growth curves for early determination of antifungal drug resistance of filamentous fungi, J. Clin. Microbiol. 40 (2013) 4718, https://doi.org/10.1128/JCM.41.10.4718-4725.2003.
[46] H.S. El-Beltagi, O.M. El-Mahdy, H.I. Mohamed, A.E. El-Ansary, Antioxidant, antimicrobial, and anticancer activities of purified chitinase of *Talaromyces funiculosus* strain CBS 129594 biosynthesized using Crustacean bio-wastes, Agron 12 (2022) 2818, https://doi.org/10.3390/agronomy12112818.
[47] M. Kumari, S. Taritla, A. Sharma, C. Jayabaskaran, Antiproliferative and antioxidative bioactive compounds in extracts of marine-derived endophytic fungus *Talaromyces purpureogenus*, Front. Microbiol. 9 (2018) 1777, https://doi.org/10.3389/fmicb.2018.01777.
[48] R.C. Mishra, R. Kalra, R. Dilawari, S.K. Deshmukh, C.J. Barrow, M. Goel, Characterization of an endophytic strain *Talaromyces assiutensis*, CPEF04 with evaluation of production medium for extracellular red pigments having antimicrobial and anticancer properties, Front. Microbiol. 12 (2021), 665702, https://doi.org/10.3389/fmicb.2021.665702.
[49] K. Ganesan, A. Manivel, Evaluation of anticancer activity of squalene isolated from *Canthium coromandelicum* leaves, World J. Pharm. Res. 7 (2018) 642–648.
[50] M. Nazemi, A. Motallebi, E. Abbasi, M. Khaledi, M. Zare, Antibacterial, antifungal, and cytotoxic activity of the fraction contains squalene in the acetone extract of a sea cucumber, Stichopus hermanni. Iran. J. Fish. Sci. 21 (2022) 1495–1507.
[51] M.Y. Alfaifi, T.M.M. Abuamara, M.E. Amer, M.S.M. Nasr, W.M. Abd-Elhay, L.E. Ei-Moselhy, T.A. Gomah, S.E.I. Elbehairi, H.A. Ali, A.F. Mohamed, Use of secondary metabolites derived from *Aspergillus* species as anticancer agents and related histological and genetic alterations: *in vitro* study, J. Cytol. Histol. 11 (2020) 1, https://doi.org/10.37421/jch.2020.11.552.
[52] V. Nguyen, J.S. Lee, Z. Qian, Y. Li, K. Kim, S. Heo, Y. Jeon, W.S. Park, I. Choi, J. Je, W. Jung, Gliotoxin isolated from marine fungus *Aspergillus* sp. induces apoptosis of human cervical cancer and chondrosarcoma cells, Mar. Drugs 12 (2014) 69, https://doi.org/10.3390/md12010069.